

# Thermo-mechanical strengthening mechanisms in a stable nanocrystalline binary alloy – A combined experimental and modeling study

C. Kale<sup>a</sup>, S. Turnage<sup>a,b</sup>, P. Garg<sup>a</sup>, I. Adlakha<sup>a,c</sup>, S. Srinivasan<sup>a</sup>, B.C. Hornbuckle<sup>b</sup>, K. Darling<sup>b</sup>, K.N. Solanki<sup>a,\*</sup>

<sup>a</sup> School for Engineering of Matter, Transport, and Energy, Arizona State University, Tempe, AZ 85287, USA

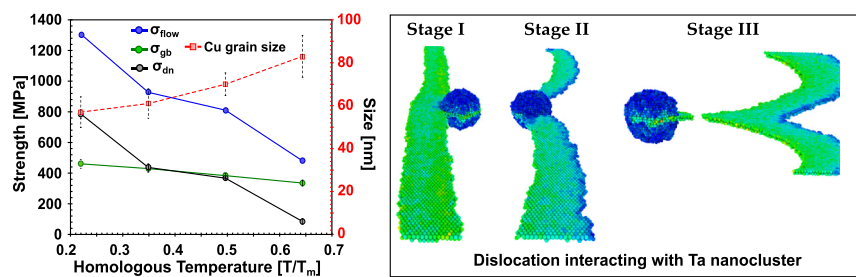
<sup>b</sup> Weapons and Materials Research Directorate, Aberdeen Proving Ground, MD 21005, USA

<sup>c</sup> Department of Applied Mechanics, Indian Institute of Technology - Madras, Chennai, India

## HIGHLIGHTS

- Nanocrystalline (NC) Cu-Ta alloy exhibits superior stability and high temperature strength compared to other NC materials.
- Grain boundary mediated dislocations interacting with nanocluster govern majority of the strength exhibited by the alloy.
- Kinetic stabilization of the microstructure aids in the development of advanced NC materials for extreme applications.

## GRAPHICAL ABSTRACT



## ARTICLE INFO

### Article history:

Received 18 October 2018

Received in revised form 2 December 2018

Accepted 13 December 2018

Available online 15 December 2018

### Keywords:

Nanocrystalline

Deformation

Transmission electron microscopy

Atomistic

## ABSTRACT

An immiscible nanocrystalline (NC) copper-tantalum (Cu-Ta) alloy is shown to exhibit a stable microstructure under thermo-mechanical loading conditions with exceptional mechanical strength (i.e., 1200 MPa strength at 298 K) indicating anomalous deformation mechanisms as compared to microstructurally unstable nanocrystalline materials. Therefore, in this work, various aspects of strength partitioning in such NC Cu-Ta alloys are discussed and the role of tantalum nanoclusters on the dominant deformation mechanism is presented as a function of temperature. Toward this, initially, the mechanical responses of NC Cu-Ta alloy were measured under uniaxial compression experiments at various temperatures. Later, atomistic simulations were performed along with the high-resolution electron microscopy to identify and validate the rate limiting mechanism behind the plastic deformation in NC Cu-Ta alloys. In general, the observed trend through experiments and simulations identify a transition from a dislocation – nanocluster interaction mediated deformation mechanism to one controlled by grain boundary strengthening as the temperature increases. The former mechanism is shown here to have a crucial role in the observed strengthening behavior of microstructurally stable NC materials. Overall, the paper demonstrates that through effective nano-engineering techniques, it is expected to extend the scope of nanocrystalline materials to a number of engineering design applications.

© 2018 Elsevier Ltd. This is an open access article under the CC BY-NC-ND license (<http://creativecommons.org/licenses/by-nc-nd/4.0/>).

## 1. Introduction

Nanocrystalline (NC) alloys exhibit enhanced static strength compared to coarse-grained and hence garner a significant interest

in unraveling various deformation mechanisms, such as grain rotation and growth [1–8]. These types of grain boundary diffusional mechanisms (grain rotation and growth) require less flow stress than matrix mediated dislocation mechanisms at such small grain sizes (i.e. <100 nm) [9]. Simulations and experimental observations in addition to in-situ and ex-situ electron microscopy (TEM) studies have been instrumental in contributing to a general understanding

\* Corresponding author.

E-mail address: [kiran.solanki@asu.edu](mailto:kiran.solanki@asu.edu) (K.N. Solanki).

of the deformation mechanisms operating in NC materials at moderately low homologous temperatures [10–17]. For instance, atomistic studies have revealed that grain boundaries (GBs) serve as the source for dislocation nucleation and also provide a point for storage and annihilation/absorption of dislocations after they transverse the grain under an applied stress [18]. These GBs are also responsible for pinning the dislocations ultimately obstructing their motion by strongly influencing when and where cross-slip can occur and by increasing the energy to unpin and move across to the neighboring grains [18,19]. In the case of CG metals, the movement of the dislocations and their interaction with microstructural features such as solutes, precipitates and GBs contribute significantly to the plastic deformation [20]. However, certain NC metals have shown limited room temperature plasticity [21,22]. Limited dislocation activity has led to modes such as twinning in NC alloys and GB rotation/sliding in NC metals [8,23–27]. Additionally, deformation mechanisms in NC metals and alloys are not only dependent on the material properties but also external variables such as the mode and or rate of loading. The expression of such has led to many fascinating and unanticipated responses of NC materials, such as strain rate sensitivity [28], low temperature super-plasticity [29–31] and creep [32–35].

Despite significant advancements in knowledge related to the plastic deformation in NC materials, there still remains a considerable gap in the understanding of how NC materials will respond if the underlying microstructure is stable. In other words, the possible deformation mechanisms that can contribute to superior strength need to be determined when predominate deformation mechanisms, grain rotation and growth, are prevented i.e. the microstructure is stabilized. Intensive research efforts on kinetically stable nanocrystalline alloys have led to the fabrication of stable Cu-Ta alloys [28,36–41]. The stability of these alloys stems from the thermal decomposition of non-equilibrium solid solutions and the formation of a Ta based nano-clusters [42,43]. The formation of these stabilized clusters is directly responsible for preventing grain growth in the presence of thermal and/or mechanical stimulus [9]. Specifically, one such alloy, NC-Cu-10 at.% Ta, is produced through ball milling followed by equal channel angular extrusion (ECAE) [28,36–40,44], (referred to as NC Cu-Ta hereafter). This particular alloy, for the past few years, has been the focus of several research articles that collectively develop a basic understanding of its unique features and response. For instance, the NC Cu-Ta alloy has shown an ability to retain a nanocrystalline grain size after exposure to 97% of its melting point combined with severe plastic deformation (450% strain) [40]. Also, the NC-Cu-10 at.% Ta alloy shows the exceptional mechanical behavior expected of a nanocrystalline material with compressive yield strengths in excess of 1000 MPa at room temperature [39]. While much of the present experimental work has, as a first step, detailed the structure and mechanical properties, the complex nature of the microstructure has prevented delineating the specific mode or modes of deformation operating in these systems.

In this work, mechanical compression experiments at different temperatures along with HRTEM and atomistic simulations are used to elucidate the strengthening behavior of such stable alloys. Atomistic simulations along with a theoretical analysis of the experimental data reveal that the dislocation interacting with the Ta based atomic clusters dominate the alloy's strength up to 50% of the absolute melting temperature ( $T_M$ ) of the alloy. Further, at temperatures beyond 50% of the  $T_M$ , increased coherency of the Ta nanoclusters with the Cu matrix at higher temperatures reduces the strengthening contribution from the dislocation interacting with Ta nanoclusters.

## 2. Experimental details

The Cu-Ta alloy was produced using cryogenic ball milling of powders followed by ECAE at 700 °C. Further details of the ball milling and ECAE process can be found elsewhere [40]. To characterize the thermo-mechanical response of the alloy, quasi-static compression

experiments were performed over a temperature range of room temperature (298 K) to 1073 K. Quasi-static compression testing was performed using an electro-mechanical load frame and a clam-shell furnace rated up to 1100 °C. The loading rods were machined from INCONEL, which maintains excellent mechanical properties at elevated temperature. Non-metallic lubricant was used to minimize friction effects at high temperature. The specimens were maintained at the test temperature for 30 min to attain thermal equilibrium. The temperature was monitored by K-type thermocouples directly attached to the loading rods close to the specimen. Once thermal equilibrium was achieved, the samples were then loaded with a strain rate of  $0.01 \text{ s}^{-1}$ . Upon completion of the mechanical testing, samples were immediately quenched in the room temperature water to freeze the underlying microstructure.

HRTEM was performed using a JEOL ARM-200F microscope operated at 200 keV. TEM samples were prepared by punching a 3 mm disk from the as-received as well as post-deformed samples and thinning them up to a thickness of approximately 70–80  $\mu\text{m}$ . Following grinding, the samples were dimpled to a roughly 5  $\mu\text{m}$  thickness. To obtain electron transparent regions, the dimpled sample where ion milled using A Gatan precision ion polishing system. To minimize contamination of the TEM foils, plasma cleaning was performed prior to TEM experiments. Approximately 600 grains were used for each specimen to calculate grain size and other measurements for reliable statistics.

## 3. Computational details

The large-scale atomic/molecular massively parallel simulator (LAMMPS) was used to perform atomistic simulations [45] using the angular-dependent potential (ADP) for the Cu-Ta alloy [46]. To calculate the strength obtained from the dislocation interacting with a Ta nanocluster, an edge dislocation was introduced in a cuboidal box of copper atoms with X-axis, Y-axis and Z-axis oriented along the  $[1\bar{1}0]$ ,  $[11\bar{2}]$  and  $[111]$ , respectively, as described by Bhatia et al. [47,48]. Based on the convergence studies, the simulation cell size of  $160b \times 160b \times 80b$  with  $\sim 2.5$  million atoms were chosen to ensure that the simulation cell is sufficiently large to assess the steady-state dislocation velocity ( $b = 2.556 \text{ \AA}$ ). Please see appendix Fig. A1 for schematic of the initial simulation setup. To simulate dislocation motion, periodic boundary conditions were prescribed along the  $[1\bar{1}0]$  (Burger's vector direction) and  $[111]$  (dislocation line direction); while, a free boundary condition was maintained along the  $[11\bar{2}]$  (slip plane normal). The edge dislocation dissociated into two partials with a stacking fault width of 3.5 nm after the conjugate-gradient relaxation for 1 ns, which is found to be in good agreement with the reported literature values of 3.0–3.6 nm for copper [49]. A 4 nm diameter tantalum nanocluster was introduced in a copper nanocrystal 8 nm away from the dislocation and the model was equilibrated using an NVT ensemble. The orientation relation between the Cu matrix and Ta nanocluster was  $d_{\text{Cu}}\{111\} \parallel d_{\text{Ta}}\{110\}$  (see [38]). The equilibrated atomistic model of copper atoms containing an edge dislocation (8 nm line length) and a Ta nanocluster (4 nm diameter) was sheared in the X-direction to simulate dislocation glide. The top and bottom regions ( $\sim 10 \text{ \AA}$ ) along the Y-direction were fixed. A shear strain rate of  $10^8 \text{ s}^{-1}$  was applied to the top of the simulation box along the X-direction to simulate dislocation glide and calculate dislocation-nanocluster strengthening ( $\sigma_{dn}$ ) at the desired temperatures. Enough relaxation time was provided after each loading step in order to avoid any superficial effects of strain rate on the dislocation interaction with nanoclusters.

## 4. Results and discussion

The primary microstructure characterization of the as-received NC Cu-Ta alloy is presented in Fig. 1. Note that in our previous work, atom probe tomography characterization of the NC Cu-Ta alloy have showed

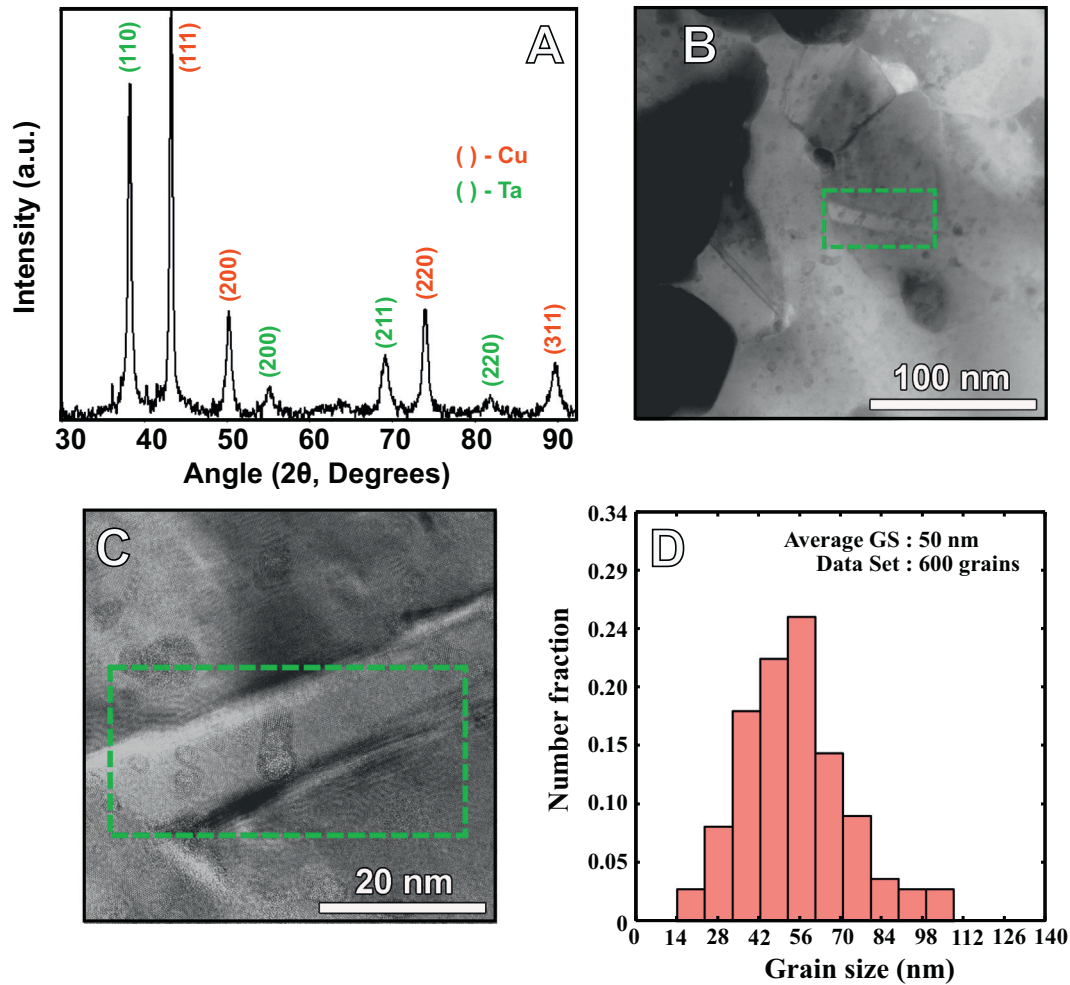


**Fig. 1.** (A) XRD peaks for as-received NC Cu-Ta alloy. (B) BFSTEM image of as-received NC Cu-Ta alloy microstructure. (C) As-received HRTEM image of NC Cu-Ta alloy highlighting the segregation of Ta nano-clusters within the microstructure. (D) As received, grain size distribution for Cu.

minimal concentrations of O and Fe contaminations and thus resulting in a high purity alloy [28]. Nonetheless, X-ray diffraction (XRD) measurements, as shown in Fig. 1A, identified the presence of a binary phase separated alloy consisting of Cu and Ta phases. Bright field scanning TEM (BF-STEM) images reveal a mean Cu (bright phase) grain size of  $50 \pm 17.5$  nm and a bimodal distribution for Ta (dark phase), see Fig. 1B. Ta is present as either nano-sized clusters (size  $<14$  nm) or larger particles (size  $>14$  nm). Higher magnification TEM images (Fig. 1C) indicate a large number of coherent or semi-coherent Ta based nano-clusters having a mean cluster size of  $3.2 \pm 0.9$  nm with an average effective inter-cluster spacing of  $5.23 \pm 1.74$  nm. The coherency of these nanoclusters along with average misfit strain at the interface can be found in our previous work, see [38]. These nanoclusters are widely distributed within the Cu grains as well as along GBs and twin boundaries. The number density of these nanoclusters was found to be  $6.25 \times 10^{23} \text{ m}^{-3}$  through atom probe tomography characterization [28]. Fig. 1D provides the distribution of the Cu grain sizes calculated over 600 grains.

Next, uniaxial-compression experiments were conducted to measure the stress-strain response of NC Cu-Ta alloy at different temperatures. Fig. 2 provides the mechanical response of the alloy at different temperatures. The compressive stress-strain curves (Fig. 2) display a nearly elastic-perfectly plastic behavior over the temperature range examined here with no substantial strain hardening. Additionally, NC Cu-Ta alloy exhibits room temperature yield strength of about 1100 MPa and 10% flow strength of 1307 MPa. The room temperature

yield strength for NC Cu-Ta alloy is almost 2 times that of pure NC Cu with comparable grain size [50]. Similarly, at 473 K, the alloy maintained 10% flow strength of almost 1000 MPa. Furthermore, the compressive yield strength of NC Cu-Ta alloy at 80% of its melting

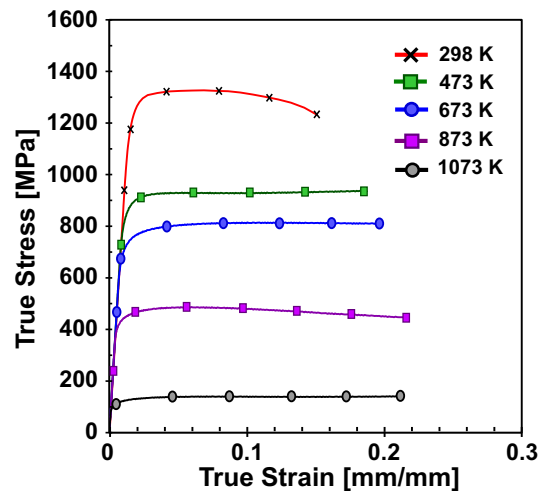


**Fig. 2.** Compression mechanical response of nanocrystalline Cu-Ta alloy subjected to a strain rate of  $0.01 \text{ s}^{-1}$  at different temperatures.

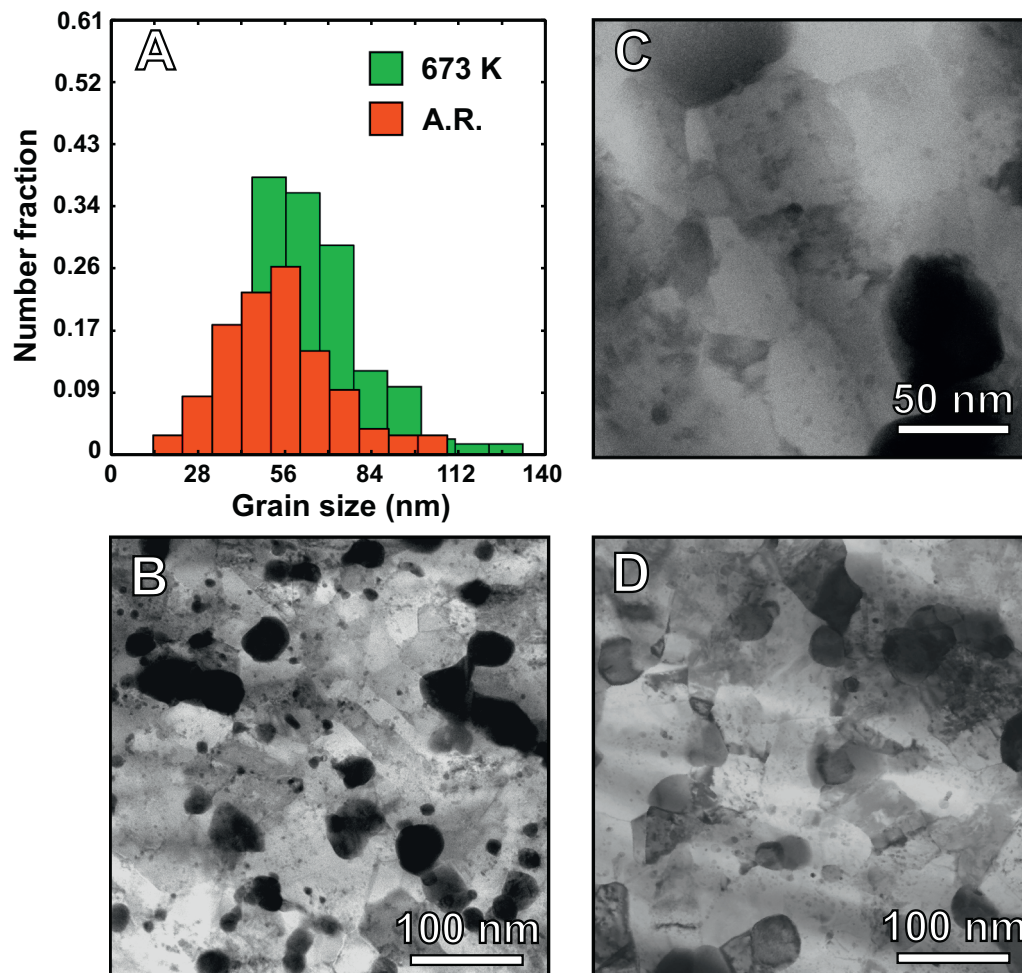


Fig. 3. (A) Number distributions for Cu grain size. Post deformed bright field STEM image of NC Cu-Ta alloy tested at (B) 473 K (C) 873 K and (D) 1073 K.

temperature is  $>3$  times the strength of pure polycrystalline Cu and same as that of pure polycrystalline brass at 298 K [51]. Such stable mechanical behavior at elevated temperature is not typical for a nanocrystalline system [52–55]. Furthermore, we know that diffusional-flow is inversely-proportional to the mean grain size. Therefore, maintaining such a high strength at  $0.8 T_m$  marks a significant deviation from the usual expectation.

Post-deformation characterization at various temperatures was performed to assess the changes in the microstructure, see Fig. 3. Fig. 3A shows that the marginal changes in grain size after testing at the strain rate of  $0.01 s^{-1}$  at 673 K ( $0.5 T_m$ ), as compared to as-received is within the error of statistical measurements. Similarly, at 1073 K, the post-deformed grain size (not shown here) was observed to be  $89.7 \pm 12.8$  nm. Fig. 3B–D provides STEM images of the post-deformed microstructure of NC Cu-Ta alloy tested at 473 K, 873 K, and 1073 K. It is evident from the BF STEM images that while the grain size increases slightly, the alloy maintains a nanocrystalline grain size even after deformation at temperatures as high as  $0.8 T_m$ . From this, it is clear that the NC Cu-Ta alloy shows dramatic microstructural stability despite being exposed to temperatures above the consolidation temperature of 973 K. Previous experimental and modeling work on Cu-Ta alloys [36,38] have shown that the extremely stable segregated Ta nanoclusters within the grains and along the grain boundaries provide pinning of grain boundaries under the application of thermo-mechanical conditions, resulting in a minimal increase in the Cu grain size [9]. Therefore, considering the relatively small change in the average grain size (i.e., the underlying microstructure is same); the likelihood of deformation mechanisms governed by dislocation motion

versus grain boundary strengthening is explored next through atomistic simulations and theoretical analysis.

The BF STEM image of a post-deformed sample tested at 673 K in Fig. 4A shows dislocations pinned around multiple Ta nanoclusters. This indicates that the Ta nanoclusters serve as pinning sites to prevent dislocation motion through a grain in addition to grain boundary pinning. Similar evidence of dislocations interacting with Ta nanoclusters (not shown here) were observed in the post-deformed TEM images for samples tested at temperatures ranging from 298 K up to 1073 K. At finer length scales ( $<100$  nm), as in the case of NC Cu-Ta alloy presented here, dislocations emitted from grain boundary sources (i.e., grain boundary dislocation) glide across the grain under the application of stress and tend to interact with the nanoclusters. On the contrary, for coarse grained material, lattice dislocations interact with the second phase particles resulting in Orowan-type strengthening mechanisms with an appreciable strain hardening. Therefore, it stands to reason that the interaction of grain boundary dislocations with the Ta nanoclusters should partially contribute to the strength of the alloy at different temperatures. To estimate the stress associated with dislocation–nanocluster interaction strengthening ( $\sigma_{dn}$ ), atomistic simulations were performed at 298 K and 473 K and the results are discussed below. Note that the interface orientation relationship between Cu and Ta nanocluster obtained through experiments were considered in the atomistic simulations, see [38].

Atomistic simulations reveal that during the shear process, the edge dislocation glides in the perfect crystal until it meets and gets pinned at the Ta nanocluster, see Fig. 4 (as shown in stage I). The dislocation bows around the Ta nanocluster with an increase in shear strain in

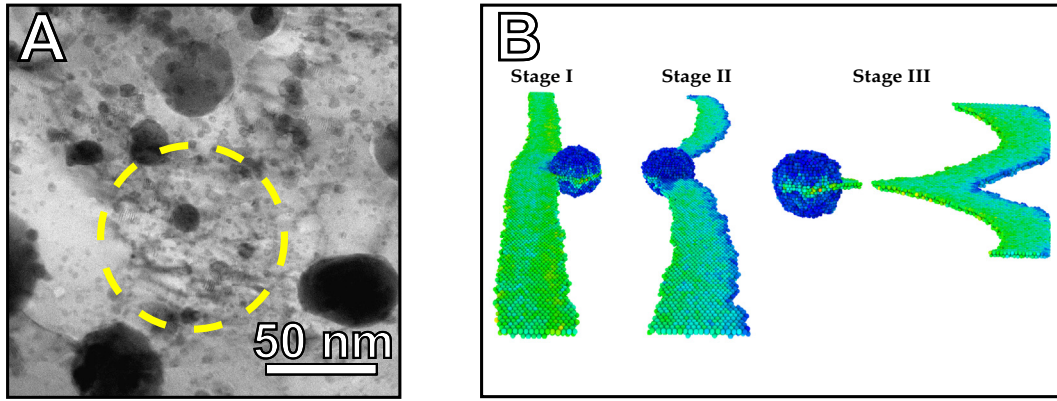


**Fig. 4.** (A) Post-deformed bright field STEM (BF STEM) image of NC Cu-Ta alloy deformed at 673 K showing dislocations pinned by multiple Ta nanoclusters. (B) Series of snapshots at different time steps from atomistic simulations showing the pinning of the dislocation (Stage I), interaction of the dislocation with the Ta nanocluster (Stage II) and breaking away of the dislocation (Stage III). Only the spherical Ta nanocluster and the edge dislocation in the Cu matrix are shown for better visibility using the atomic strain analysis. The atoms are color coded according to the shear strain,  $\gamma_s$ , ranging from 0.0 to 0.5.

stage II, similar to the observed bowing of the dislocation around Ta nanoclusters in the TEM image (Fig. 4A). The stress required for dislocation glide corresponding to the applied shear strain is calculated at each step based on the elastic properties of NC Cu-Ta alloy. As the shear strain is increased further, the dislocation breaks away from the Ta nanocluster in stage III and again glides in the perfect crystal (Fig. 4B). Therefore, the stress required to break the dislocation away from the Ta nanocluster in stage III gives a measure of the dislocation-nanocluster strengthening. From the atomistic simulations, the value of  $\sigma_{dm}$  was found to be 867 MPa and 695 MPa at 298 K and 473 K, respectively. The dislocation-nanocluster strength obtained from atomistic simulations, 867 MPa, at 298 K amounts to considerable portion of the experimental flow strength of 1307 MPa. Same is true for the results at 473 K. These results indicate that at low to moderately high temperatures, the Ta nanoclusters play a significant role in the deformation mechanism by acting as obstacles to the dislocation motion. Due to limitations of the computational setup, it is slightly difficult to discern the role of Ta nanoclusters at higher temperatures. Hence, a theoretical route was used to understand further the dislocation-nanocluster strengthening at different temperatures, which is discussed below.

In order to understand the underlying mechanisms contributing to the remarkable strength, a theoretical analysis based on the experimental results was performed. Note that in previous work on NC Cu-Ta alloy, Darling et al. [40] have shown that the exceptional room temperature strength of this alloy is a complex function of grain boundary strengthening as well as different strengthening mechanisms rendered by the Ta nanoclusters. In this work, we revisit some of the strengthening mechanisms presented in [40] while providing a detailed breakdown of strength observed in NC Cu-Ta alloy at temperatures as high as 873 K (0.65  $T_m$ ). For nanocrystalline materials, strengthening due to grain boundaries, i.e., the Hall-Petch strengthening, under room temperature conditions can be computed from:

$$\sigma_{gb} = kd^{-1/2} \quad (1)$$

where  $k$  is a material parameter with a value of 0.110 MPa-m<sup>1/2</sup> for NC Cu-Ta alloy [40] and  $d$  is the mean grain size. However, in order to determine the strengthening contribution of grain boundaries at higher temperatures, a correction factor must be applied along the lines of:

$$\sigma_{gb}(T) = \left(\frac{G(T)}{G_0}\right)^{1/2} kd^{-1/2} \quad (2)$$

where  $G_0$  and  $G(T)$  are the shear modulus at 298 K and the desired temperature, respectively [56]. The grain boundary strength  $\sigma_{gb}$  calculated from Eq. (2) is shown in Fig. 5A for various temperatures. The

contribution from  $\sigma_{gb}$  remains fairly constant (green curve in Fig. 5A) from 298 K (0.22  $T_m$ ) to 873 K (0.65  $T_m$ ). This behavior can be attributed to the hitherto microstructure stability exhibited by the alloy.

At 298 K, it can be seen that  $\sigma_{gb}$  is 461 MPa, which contributes only 35% of the observed flow stress ( $\sigma_{flow}$ ). To account for the remaining strength of the material, we also determine the frictional stress in pure Cu ( $\sigma_o$ ), which is about 20 MPa (constant at all temperatures). The rule of mixtures strength ( $\sigma_{ROM}$ ) given by:

$$\sigma_{ROM} = V_{ppt} \left[ H_{ppt} - \left( \frac{H_{HP}}{1000} \right) \right] \quad (3)$$

where  $V_{ppt}$  is the volume fraction of Ta nanoclusters, and  $H_{ppt}$  and  $H_{HP}$  are the hardness of the Ta nanoclusters (4.1 GPa) and the hardness from the Hall-Petch effect, respectively [40] contribute about 40 MPa for all temperatures. After accounting for  $\sigma_{gb}$ ,  $\sigma_o$ , and  $\sigma_{ROM}$ , still almost 65% of the room temperature flow stress, which is about 786 MPa, should come from a secondary strengthening mechanism. Similarly, at 473 K and 673 K the contributions from  $\sigma_{gb}$ ,  $\sigma_o$  and  $\sigma_{ROM}$  result in just 50% of the observed flow stress at those temperatures. Thus, the secondary strengthening mechanism should account for the remaining 50% of the flow strength at 473 K and 673 K, which are 437 MPa and 367 MPa, respectively. This contribution is almost equivalent to the contribution obtained from the grain boundary strengthening at those temperatures. However, at 873 K (0.65  $T_m$ ), the contribution from the secondary strengthening source falls below the grain boundary strengthening. In other words, results underscore a transition from a dislocation interaction with nanoclusters controlled deformation mechanism to one controlled by grain boundary at elevated temperatures.

The numerical values obtained from the atomistic simulations of dislocation interaction with nanocluster are 867 MPa and 695 MPa at 298 K and 473 K, respectively. These values are in the same order as estimated above using the theoretical analysis of the experimental flow stresses (786 MPa and 437 MPa at 298 K and 473 K). However, the variation between experiments and atomistic simulations could be due to the fact that the effective dislocation glide resistance in experiments is likely to be a complex function of dislocation characters. Further, the results from atomistic simulations could be regarded as an upper bound due to the limited complexity of the atomistic model as compared to the experiments. Nevertheless, reasonable estimates for secondary strengthening obtained using both atomistic simulations and experiments indicate that the remaining contributions to the flow stress come from the dislocation-nanocluster interactions. Further, the TEM micrographs of the post-deformed samples (at all tested temperatures, e.g. Fig. 4A) strongly indicate that the dislocations do interact with the Ta. However, in terms of strength contributions, such interaction was found to be

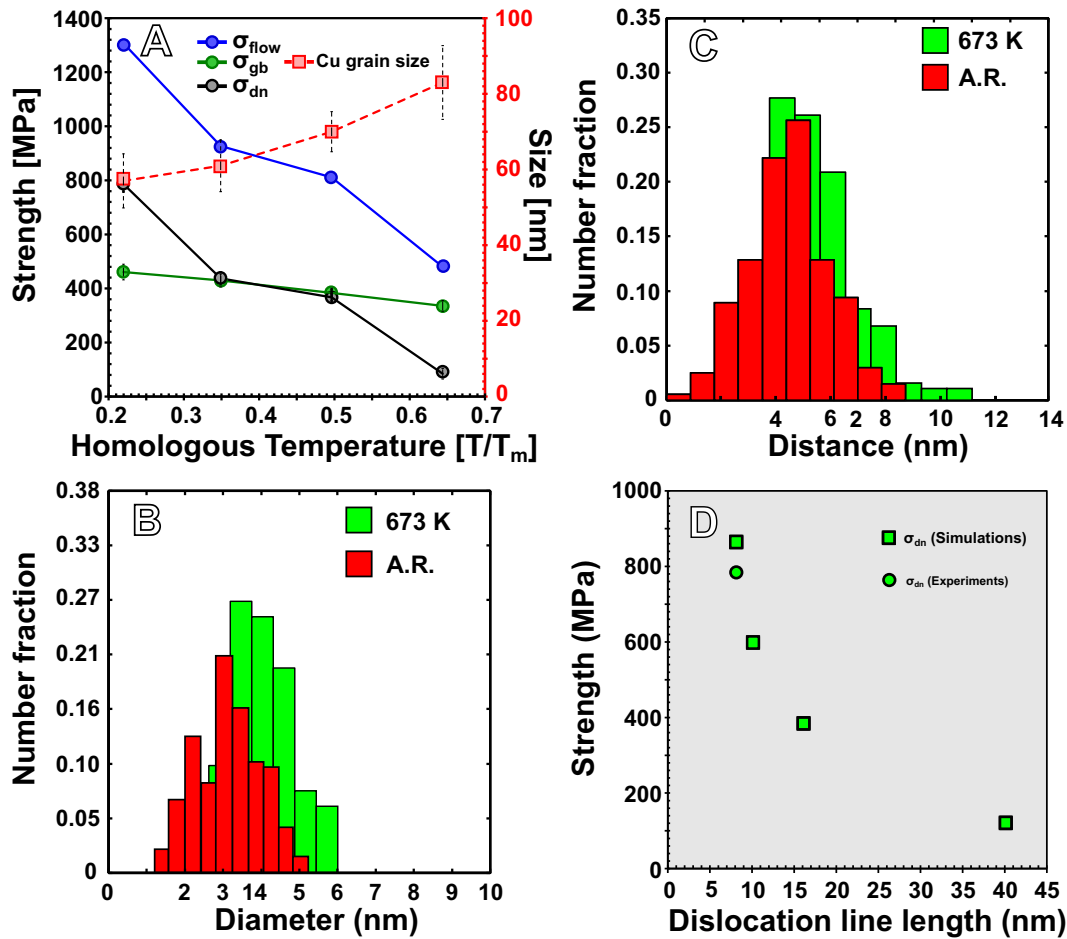


**Fig. 5.** (A) Flow strength ( $\sigma_{flow}$ , flow stress at 10% strain from Fig. 2), temperature corrected grain size strengthening ( $\sigma_{gb}$ ), dislocation-nanocluster strength ( $\sigma_{dn}$ ) on primary Y-axis (left side) and post-deformed Cu grain size on secondary Y-axis (right side) plotted as a function of homologous temperature. The error bars for  $\sigma_{dn}$ ,  $\sigma_{gb}$ , and Cu grain size represent one standard deviation. Number distribution for (B) Ta cluster size and (C) Ta inter-cluster spacing for as-received and sample tested at 673 K. (D) Dislocation – nanocluster strength obtained from atomistic simulations plotted against different dislocation line lengths at 298 K.

relatively insignificant (green line in Fig. 5A) compared to the Hall-Petch relationship (black line in Fig. 5A). That is, at higher temperatures, the dislocation – nanocluster strength starts to fall behind, and the grain boundary contribution dominates the strength. To summarize, at 298 K, the dislocation–nanocluster strengthening dominates over the grain boundary strengthening mechanisms. At moderate temperatures, there is equal contribution from the dislocation–nanocluster interaction and the grain boundary strengthening. Finally, at higher temperatures, the strength of the NC Cu-Ta alloy is governed by the Hall-Petch relationship.

The size distribution of Ta nanoclusters post-deformation is also plotted in Fig. 5B, show a statistically insignificant coarsening as their average size changes from  $3.2 \pm 0.9$  nm in the as-received condition to about  $4.1 \pm 1.3$  nm in the sample deformed at 673 K ( $0.5 T_m$ ). Furthermore, there is a marginal change in the inter-cluster spacing of the Ta nanoclusters as seen in Fig. 5C. The extreme statistics of Ta nanocluster spacing observed is between an average of 4 nm in the as-received condition to 9 nm for sample tested at 873 K. Therefore, to quantify the effects of change in the dislocation line length, atomistic simulations were also performed at 298 K for different dislocation line lengths ranging from 8 nm to 40 nm. From Fig. 5D, it can be seen that the dislocation-nanocluster strength obtained for dislocation line length of 8 nm and 10 nm is 867 MPa and 601 MPa, respectively, which is comparable to the experimentally observed value of 786 MPa.

It is worth noting that the decrease in the  $\sigma_{dn}$  as the temperature increases can be attributed to the change in lattice misfit strain between

the Cu matrix and the Ta nanoclusters. In previous in-situ TEM work by Rajagopalan et al. [38] on the same NC Cu-Ta alloy, it has been shown that the average lattice misfit strain changes approximately from  $12.9\% \pm 2\%$  at 298 K to about 4% at 673 K. Further, the lattice misfit strain obtained using atomistic simulations (15%) compare reasonably well with the experimentally calculated value (13%) at 298 K, see [38]. At lower temperatures, the semi-coherent interface of the Ta nanoclusters forms a strong resistance for the dislocation to bypass under an applied stress. However, with increasing temperature, the misfit strain relaxes, and the Ta nanoclusters become more coherent, thereby, allowing easier bypass of dislocations. Hence, a very large effect of dislocation-interaction with nanocluster at lower temperatures is prevalent as compared to the grain boundary strengthening. Therefore, the drop in the average misfit strain nearly correlates with the drop in the contribution obtained from the  $\sigma_{dn}$  as the temperature is increased from 298 K to 673 K. Overall, the combined results from the TEM micrographs and the atomistic simulations lead to the conclusion that dislocation-nanocluster ( $\sigma_{dn}$ ) strengthening accounts for the remaining strengthening mechanism in the NC Cu-Ta.

## 5. Conclusion

In summary, the mechanical behavior of cryomilled NC Cu-Ta alloy was investigated as a function of temperature ranging from 298 K to 1073 K. Furthermore, HRTEM and atomistic simulations were utilized to understand the breakdown of strength observed in a truly stable

nanocrystalline system at different homologous temperatures. The results show that NC Cu-Ta alloy showed negligible grain coarsening under thermo-mechanical loading and as a result the strength due to grain refinement remained more or less constant for all temperatures tested. Also, at 298 K, the strength due to dislocations interacting with Ta nanoclusters contributes almost 65% of the alloy's strength. Furthermore, at 473 K and 673 K, strength obtained from dislocation-nanocluster interaction is equivalent to the grain boundary strengthening. We conclude that along with grain boundary strengthening, dislocation-nanocluster ( $\sigma_{dn}$ ) strengthening contributed to the observed experimental strength of the alloy. Overall, this study provides an insight into the temperature dependent mechanical behavior of a new class of truly stable nanocrystalline alloys. From a broader perspective, the present work demonstrates that in a kinetically stabilized NC materials, nano - second phases or nano - precipitates could play equal or larger role in overall contribution to the strengthening behavior as compared to the grain boundary strengthening, which is a predominant strengthening mechanism in the thermodynamically stable nanocrystalline system (e.g. [57]). Furthermore, introduction of such phases could also suppress the plastic instability (reduced dislocation avalanche) typically observed in NC materials [58].

### CRedit authorship contribution statement

**C. Kale:** Data curation, Formal analysis, Writing - review & editing. **S. Turnage:** Data curation. **P. Garg:** Data curation, Writing - review & editing. **I. Adlakha:** Data curation. **S. Srinivasan:** Data curation. **B.C. Hornbuckle:** Data curation, Formal analysis. **K. Darling:** Conceptualization, Formal analysis, Writing - review & editing, Supervision. **K.N. Solanki:** Conceptualization, Formal analysis, Writing - review & editing, Supervision.

### Acknowledgements

This work was supported by the US Army Research Laboratory and the National Science Foundation under grants W911NF-15-2-0038 and 1663287, respectively.

### Data availability

Data generated or analysed that support the findings are available from the corresponding author on reasonable request.

### Appendix A

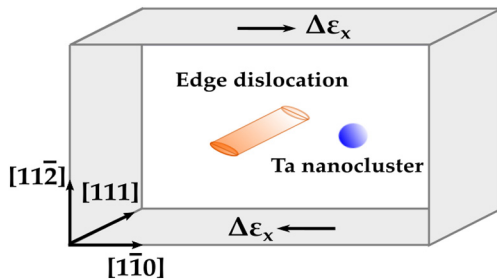


**Fig. A1.** Schematic of the simulation setup showing an edge dislocation and a Ta nanocluster in a single Cu nanocrystal where X, Y and Z correspond to  $[1\bar{1}0]$ ,  $[11\bar{2}]$  and  $[111]$  directions respectively.

### References

- [1] Y.M. Wang, A.V. Hamza, E. Ma, Temperature-dependent strain rate sensitivity and activation volume of nanocrystalline Ni, *Acta Mater.* 54 (2006) 2715–2726, <https://doi.org/10.1016/j.actamat.2006.02.013>.
- [2] A.H. Chokshi, A. Rosen, J. Karch, H. Gleiter, On the validity of the hall-petch relationship in nanocrystalline materials, *Scr. Metall.* 23 (1989) 1679–1683, [https://doi.org/10.1016/0036-9748\(89\)90342-6](https://doi.org/10.1016/0036-9748(89)90342-6).
- [3] C. Duhamel, Y. Brechet, Y. Champion, Activation volume and deviation from Cottrell–Stokes law at small grain size, *Int. J. Plast.* 26 (2010) 747–757, <https://doi.org/10.1016/j.ijplas.2009.10.003>.
- [4] Y.T. Zhu, X.L. Wu, X.Z. Liao, J. Narayan, L.J. Kecskés, S.N. Mathaudhu, Dislocation–twin interactions in nanocrystalline fcc metals, *Acta Mater.* 59 (2011) 812–821, <https://doi.org/10.1016/j.actamat.2010.10.028>.
- [5] J. Li, T. Suo, C. Huang, Y. Li, H. Wang, J. Liu, Adiabatic shear localization in nanostructured face centered cubic metals under uniaxial compression, *Mater. Des.* 105 (2016) 262–267.
- [6] L. Zhou, J. Guo, G. Li, L. Xiong, S. Wang, C. Li, Investigation of annealing behavior of nanocrystalline NiAl, *Mater. Des.* 18 (1997) 373–377.
- [7] M. Akbarpour, H. Kim, Microstructure, grain growth, and hardness during annealing of nanocrystalline Cu powders synthesized via high energy mechanical milling, *Mater. Des.* 83 (2015) 644–650.
- [8] S. Cheng, J. Xie, A.D. Stoica, X.-L. Wang, J.A. Horton, D.W. Brown, H. Choo, P.K. Liaw, Cyclic deformation of nanocrystalline and ultrafine-grained nickel, *Acta Mater.* 57 (2009) 1272–1280, <https://doi.org/10.1016/j.actamat.2008.11.011>.
- [9] R.K. Koju, K.A. Darling, K.N. Solanki, Y. Mishin, Atomistic modeling of capillary-driven grain boundary motion in Cu-Ta alloys, *Acta Mater.* 148 (2018) 311–319, <https://doi.org/10.1016/j.actamat.2018.01.027>.
- [10] X. Yu, J. Rong, Z. Zhan, Z. Liu, J. Liu, Effects of grain size and thermodynamic energy on the lattice parameters of metallic nanomaterials, *Mater. Des.* 83 (2015) 159–163, <https://doi.org/10.1016/j.matdes.2015.06.019>.
- [11] S. Ramirez, K. Chan, R. Hernandez, E. Recinos, E. Hernandez, R. Salgado, A.G. Khitun, J.E. Garay, A.A. Balandin, Thermal and magnetic properties of nanostructured densified ferrimagnetic composites with graphene – graphite fillers, *Mater. Des.* 118 (2017) 75–80, <https://doi.org/10.1016/j.matdes.2017.01.018>.
- [12] R. Sahu, S. Anup, Molecular dynamics study of toughening mechanisms in nanocomposites as a function of structural arrangement of reinforcements, *Mater. Des.* 100 (2016) 132–140, <https://doi.org/10.1016/j.matdes.2016.03.076>.
- [13] S. Pal, M. Meraj, Structural evaluation and deformation features of interface of joint between nano-crystalline Fe–Ni–Cr alloy and nano-crystalline Ni during creep process, *Mater. Des.* 108 (2016) 168–182, <https://doi.org/10.1016/j.matdes.2016.06.086>.
- [14] M.S. Yaghmaee, H. Ahmadian Baghbaderani, Thermodynamics modeling of cohesive energy of metallic nano-structured materials, *Mater. Des.* 114 (2017) 521–530, <https://doi.org/10.1016/j.matdes.2016.10.067>.
- [15] C. Prasad, P. Bhuyan, C. Kaithwas, R. Saha, S. Mandal, Microstructure engineering by dispersing nano-spheroid cementite in ultrafine-grained ferrite and its implications on strength–ductility relationship in high carbon steel, *Mater. Des.* 139 (2018) 324–335, <https://doi.org/10.1016/j.matdes.2017.11.019>.
- [16] F. Yuan, X. Wu, Size effect and boundary type on the strengthening of nanoscale domains in pure nickel, *Mater. Sci. Eng. A* 648 (2015) 243–251, <https://doi.org/10.1016/j.msea.2015.09.071>.
- [17] X. Wu, F. Yuan, M. Yang, P. Jiang, C. Zhang, L. Chen, Y. Wei, E. Ma, Nanodomain nickel unites nanocrystal strength with coarse-grain ductility, *Sci. Rep.* 5 (2015), 11728, <https://doi.org/10.1038/srep11728>.
- [18] H. Van Swygenhoven, P.M. Derlet, A. Hasnaoui, Atomic mechanism for dislocation emission from nanosized grain boundaries, *Phys. Rev. B* 66 (2002), 024101, <https://doi.org/10.1103/PhysRevB.66.024101>.
- [19] J. Schiøtz, K.W. Jacobsen, A maximum in the strength of nanocrystalline copper, *Science* 301 (2003) 1357–1359, <https://doi.org/10.1126/science.1086636>.
- [20] J.P. Hirth, J. Lothe, *Theory of Dislocations*, Krieger Publishing Company, 1982.
- [21] G. Saada, Hall–Petch revisited, *Mater. Sci. Eng. A* 400–401 (2005) 146–149, <https://doi.org/10.1016/j.msea.2005.02.091>.
- [22] M. Legros, D.S. Gianola, K.J. Hemker, In situ TEM observations of fast grain-boundary motion in stressed nanocrystalline aluminum films, *Acta Mater.* 56 (2008) 3380–3393, <https://doi.org/10.1016/j.actamat.2008.03.032>.
- [23] B.Q. Li, M.L. Sui, B. Li, E. Ma, S.X. Mao, Reversible twinning in pure aluminum, *Phys. Rev. Lett.* 102 (2009), 205504.
- [24] X.Z. Liao, Y.H. Zhao, S.G. Srinivasan, Y.T. Zhu, R.Z. Valiev, D.V. Gunderov, Deformation twinning in nanocrystalline copper at room temperature and low strain rate, *Appl. Phys. Lett.* 84 (2004) 592–594, <https://doi.org/10.1063/1.1644051>.
- [25] Y.T. Zhu, X.Z. Liao, X.L. Wu, Deformation twinning in nanocrystalline materials, *Prog. Mater. Sci.* 57 (2012) 1–62, <https://doi.org/10.1016/j.pmatsci.2011.05.001>.
- [26] X.L. Wu, K.M. Youssef, C.C. Koch, S.N. Mathaudhu, L.J. Kecskés, Y.T. Zhu, Deformation twinning in a nanocrystalline hcp mg alloy, *Scr. Mater.* 64 (2011) 213–216, <https://doi.org/10.1016/j.scriptamat.2010.10.024>.
- [27] E. Izadi, A. Darbal, R. Sarkar, J. Rajagopalan, Grain rotations in ultrafine-grained aluminum films studied using in situ TEM straining with automated crystal orientation mapping, *Mater. Des.* 113 (2017) 186–194.
- [28] B.C. Hornbuckle, T. Rojhirunsakool, M. Rajagopalan, T. Alam, G.P.P. Pun, R. Banerjee, K.N. Solanki, Y. Mishin, L.J. Kecskés, K.A. Darling, Effect of Ta solute concentration on the microstructural evolution in immiscible Cu-Ta alloys, *JOM* 67 (2015) 2802–2809, <https://doi.org/10.1007/s11837-015-1643-x>.
- [29] O.D. Sherby, J. Wadsworth, Superplasticity—recent advances and future directions, *Prog. Mater. Sci.* 33 (1989) 169–221, [https://doi.org/10.1016/0079-6425\(89\)90004-2](https://doi.org/10.1016/0079-6425(89)90004-2).
- [30] L. Lu, M.L. Sui, K. Lu, Superplastic extensibility of nanocrystalline copper at room temperature, *Science* 287 (2000) 1463–1466, <https://doi.org/10.1126/science.287.5457.1463>.
- [31] S.X. McFadden, R.S. Mishra, R.Z. Valiev, A.P. Zhilyaev, A.K. Mukherjee, Low-temperature superplasticity in nanostructured nickel and metal alloys, *Nature* 398 (1999) 684–686, <https://doi.org/10.1038/19486>.

- [32] M.A. Bhatia, S.N. Mathaudhu, K.N. Solanki, Atomic-scale investigation of creep behavior in nanocrystalline Mg and Mg–Y alloys, *Acta Mater.* 99 (2015) 382–391, <https://doi.org/10.1016/j.actamat.2015.07.068>.
- [33] I.-C. Choi, Y.-J. Kim, M.-Y. Seok, B.-G. Yoo, J.-Y. Kim, Y. Wang, J. Jang, Nanoscale room temperature creep of nanocrystalline nickel pillars at low stresses, *Int. J. Plast.* 41 (2013) 53–64.
- [34] V. Yamakov, D. Wolf, S. Phillpot, H. Gleiter, Grain-boundary diffusion creep in nanocrystalline palladium by molecular-dynamics simulation, *Acta Mater.* 50 (2002) 61–73.
- [35] P.C. Millett, T. Desai, V. Yamakov, D. Wolf, Atomistic simulations of diffusional creep in a nanocrystalline body-centered cubic material, *Acta Mater.* 56 (2008) 3688–3698.
- [36] K.A. Darling, M. Rajagopalan, M. Komarasamy, M.A. Bhatia, B.C. Hornbuckle, R.S. Mishra, K.N. Solanki, Extreme creep resistance in a microstructurally stable nanocrystalline alloy, *Nature* 537 (2016) 378–381, <https://doi.org/10.1038/nature19313>.
- [37] M. Bhatia, M. Rajagopalan, K. Darling, M. Tschopp, K. Solanki, The role of Ta on twinnability in nanocrystalline Cu–Ta alloys, *Math. Res. Lett.* 5 (2017) 48–54.
- [38] M. Rajagopalan, K. Darling, S. Turnage, R. Koju, B. Hornbuckle, Y. Mishin, K. Solanki, Microstructural evolution in a nanocrystalline Cu–Ta alloy: a combined in-situ TEM and atomistic study, *Mater. Des.* 113 (2017) 178–185.
- [39] K.A. Darling, C. Kale, S. Turnage, B.C. Hornbuckle, T.L. Luckenbaugh, S. Grendahl, K.N. Solanki, Nanocrystalline material with anomalous modulus of resilience and springback effect, *Scr. Mater.* 141 (2017) 36–40, <https://doi.org/10.1016/j.scriptamat.2017.07.012>.
- [40] K.A. Darling, M.A. Tschopp, R.K. Guduru, W.H. Yin, Q. Wei, L.J. Kecskes, Microstructure and mechanical properties of bulk nanostructured Cu–Ta alloys consolidated by equal channel angular extrusion, *Acta Mater.* 76 (2014) 168–185, <https://doi.org/10.1016/j.actamat.2014.04.074>.
- [41] S.A. Turnage, M. Rajagopalan, K.A. Darling, P. Garg, C. Kale, B.G. Bazehhour, I. Adlakha, B.C. Hornbuckle, C.L. Williams, P. Peralta, K.N. Solanki, Anomalous mechanical behavior of nanocrystalline binary alloys under extreme conditions, *Nat. Commun.* 9 (2018), 2699, <https://doi.org/10.1038/s41467-018-05027-5>.
- [42] A.R. Kalidindi, C.A. Schuh, Stability criteria for nanocrystalline alloys, *Acta Mater.* 132 (2017) 128–137, <https://doi.org/10.1016/j.actamat.2017.03.029>.
- [43] A.R. Kalidindi, T. Chookajorn, C.A. Schuh, Nanocrystalline materials at equilibrium: a thermodynamic review, *JOM* 67 (2015) 2834–2843, <https://doi.org/10.1007/s11837-015-1636-9>.
- [44] V.H. Hammond, T.L. Luckenbaugh, M. Aniska, D.M. Gray, J.A. Smeltzer, B.C. Hornbuckle, C.J. Marvel, K.N. Solanki, T. Schmitz, K.A. Darling, An insight into machining of thermally stable bulk nanocrystalline metals, *Adv. Eng. Mater.* 0 (n.d.), doi:<https://doi.org/10.1002/adem.201800405>.
- [45] S. Plimpton, Fast parallel algorithms for short-range molecular dynamics, *J. Comput. Phys.* 117 (1995) 1–19, <https://doi.org/10.1006/jcph.1995.1039>.
- [46] G.P. Pun, K. Darling, L. Kecskes, Y. Mishin, Angular-dependent interatomic potential for the Cu–Ta system and its application to structural stability of nano-crystalline alloys, *Acta Mater.* 100 (2015) 377–391.
- [47] M.A. Bhatia, S. Groh, K.N. Solanki, Atomic-scale investigation of point defects and hydrogen-solute atmospheres on the edge dislocation mobility in alpha iron, *J. Appl. Phys.* 116 (2014), 064302, <https://doi.org/10.1063/1.4892630>.
- [48] M.A. Bhatia, X. Zhang, M. Azarnoush, G. Lu, K.N. Solanki, Effects of oxygen on prismatic faults in  $\alpha$ -Ti: a combined quantum mechanics/molecular mechanics study, *Scr. Mater.* 98 (2015) 32–35, <https://doi.org/10.1016/j.scriptamat.2014.11.008>.
- [49] H. Häkkinen, S. Mäkinen, M. Manninen, Edge dislocations in fcc metals: microscopic calculations of core structure and positron states in Al and Cu, *Phys. Rev. B* 41 (1990) 12441–12453, <https://doi.org/10.1103/PhysRevB.41.12441>.
- [50] M. Dao, L. Lu, R.J. Asaro, J.T.M. De Hosson, E. Ma, Toward a quantitative understanding of mechanical behavior of nanocrystalline metals, *Acta Mater.* 55 (2007) 4041–4065, <https://doi.org/10.1016/j.actamat.2007.01.038>.
- [51] M.A. Meyers, K.K. Chawla, *Mechanical Behavior Materials*, 2nd ed. Cambridge University Press, United Kingdom, 2008 <http://www.cambridge.org/us/academic/subjects/engineering/materials-science/mechanical-behavior-materials-2nd-edition>, Accessed date: 24 May 2017.
- [52] F.A. Mohamed, Y. Li, Creep and superplasticity in nanocrystalline materials: current understanding and future prospects, *Mater. Sci. Eng. A* 298 (2001) 1–15, [https://doi.org/10.1016/S0928-4931\(00\)00190-9](https://doi.org/10.1016/S0928-4931(00)00190-9).
- [53] M.A. Meyers, A. Mishra, D.J. Benson, Mechanical properties of nanocrystalline materials, *Prog. Mater. Sci.* 51 (2006) 427–556, <https://doi.org/10.1016/j.pmatsci.2005.08.003>.
- [54] K.S. Kumar, H. Van Swygenhoven, S. Suresh, Mechanical behavior of nanocrystalline metals and alloys, *Acta Mater.* 51 (2003) 5743–5774, <https://doi.org/10.1016/j.actamat.2003.08.032>.
- [55] P.M. Anderson, J.S. Carpenter, M.D. Gram, L. Li, Mechanical properties of nanostructured metals, in: B. Bhushan, D. Luo, S.R. Schriker, W. Sigmund, S. Zauscher (Eds.), *Handb. Nanomater. Prop.*, Springer Berlin Heidelberg 2014, pp. 495–553 [http://link.springer.com.ezproxy1.lib.asu.edu/chapter/10.1007/978-3-642-31107-9\\_20](http://link.springer.com.ezproxy1.lib.asu.edu/chapter/10.1007/978-3-642-31107-9_20), Accessed date: 11 May 2014.
- [56] J.H. Schneibel, M. Heilmaier, Hall–Petch breakdown at elevated temperatures, *Mater. Trans.* 55 (2014) 44–51, <https://doi.org/10.2320/matertrans.MA201309>.
- [57] C. Schuh, T. Nieh, H. Iwasaki, The effect of solid solution W additions on the mechanical properties of nanocrystalline Ni, *Acta Mater.* 51 (2003) 431–443.
- [58] W. Wang, Y. Zhong, K. Lu, L. Lu, D.L. McDowell, T. Zhu, Size effects and strength fluctuation in nanoscale plasticity, *Acta Mater.* 60 (2012) 3302–3309, <https://doi.org/10.1016/j.actamat.2012.03.016>.